Paper

A Simulation of Near-Field Optics : Optical Waves Through an Aperture in 3D Thick Metallic Screen by Volume Integral Equation Method

Kazuo Tanaka* Member
Mengyun Yan* Non-member
Masahiro Tanaka* Non-member

Optical near-field in the aperture in the thick metallic screen is analyzed numerically by the three-dimensional volume integral equation with Generalized Minimum Residual Method. Numerical results have been confirmed by the invariance of the results of the discretized size and reciprocity. The dependence of the scattering cross section on the thickness of the screen have been calculated. It is found that near-field distribution around the small aperture is a slightly different from Bethe's results.

Keywords : volume integral equation, near-field optics, aperture in metallic screen, three-dimensional simulation

1. Introduction

The interaction between the object and optical near-field of the aperture on the metallic screen is one of the fundamental physical process in the near-field optics (NFO) [(1),(2)]. So, the investigation of electromagnetic near-fields in the aperture in the metallic screen is very important subject of NFO. Three-dimensional (3D) analysis of electromagnetic fields in the aperture has been treated in many papers such as famous Bethe's paper [(3)]. They treated the case where the screen is the perfect conductor that has infinitely thin or finite thickness [(4)-(12)]. The scattering of electromagnetic waves by an aperture in the thick dielectric screen has not been treated in detail so far. In NFO, we must consider that the metal screen has a finite thickness and that the metal must be regarded as the dielectric medium that has complex-valued permittivity.

Recently, several works have reported calculations of optical fields around the aperture that is made on the tip of the probe in the practical NFO system by FDTD method [(13)-(15)]. In these papers, the metal coating on the probe has been treated by the dielectric of complex-valued permittivity with a finite thickness. However, the characteristics of optical fields scattered by the aperture have not been investigated in detail in these papers. The analysis of optical fields scattered by an aperture in the metallic screen with finite thickness is one of the important and fundamental problem in NFO technology.

In this paper, we perform 3D numerical simulations of the optical field scattered by an aperture in the complex-valued dielectric screen (slab) with a finite thickness by the volume integral equation [(16),(17)]. The simulation results in this paper will give the important and interesting information concerning basic characteristics of near-field scanning microscope (NSOM).

2. Volume Integral Equations

We consider the scattering problem of optical waves by an aperture in the thick metallic screen shown in Fig. 1. A small square aperture whose area is given by $a_x \times a_y$ has been made in the thick metallic screen (slab) with thickness w. The metallic screen has infinitely width and its relative complex-valued permittivity is given by $\varepsilon_1 = n_1^2$, where n_1 is the index of refraction of the metallic screen. We consider the coordinate system (x, y, z) or (r, θ, ϕ), whose origin is located at a geometrical center of the aperture on the upper surface of the screen, as shown in Fig. 1. The optical plane wave is assumed to be incident with an incident angle (θ_i, ϕ_i) from the region (I) below the metallic screen shown in Fig. 1. An aperture in the screen makes the optical near-field and makes scattering waves. When we place the small object near the aperture and measure the scattered far-field by scanning the object position along the screen surface, we can simulate the imaging procedure of the illumination-mode of the practical SNOM.

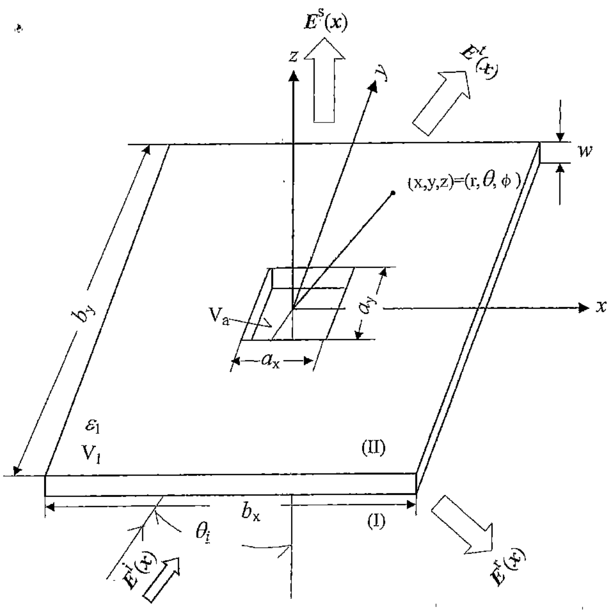

Fig. 1. Geometry of the problem

* Department of Electronics & Computer Engineering, Gifu-University
1-1, Yanagido, Gifu 501-1193

In this paper, we solve the problem shown in Fig. 1 by the volume integral (Lippman-Shwinger) equation. The volume integral equation for the problem shown in Fig. 1 can be written as

$$\boldsymbol{E}(\boldsymbol{x}) = k_0^2(n_1^2-1)\iiint_{V_1} \underline{G}_e(\boldsymbol{x}|\boldsymbol{x}')\cdot\boldsymbol{E}(\boldsymbol{x}')\mathrm{d}v' + \boldsymbol{E}^i(\boldsymbol{x}), \quad \cdots\cdots\cdots(1)$$

where $\boldsymbol{E}(\boldsymbol{x})$ is the total electric field, $\boldsymbol{E}^i(\boldsymbol{x})$ is the incident electric field given by

$$\boldsymbol{E}^i(\boldsymbol{x})=\boldsymbol{E}_0 exp[-jk_0(\mathrm{x}\sin\theta_i\cos\phi_i+\mathrm{y}\sin\theta_i\sin\phi_i+z\cos\theta_i)] \quad \cdots\cdots(2)$$

and $\boldsymbol{E}_0$ represents the incident amplitude vector. In Eq. (1) $\underline{G}_e(\boldsymbol{x}|\boldsymbol{x}')$ is an electric-type free-space dyadic (tensor) Green's function. The volume integral region V_1 represents the region of metallic screen with an aperture shown in Fig. 1. Since the integration region V_1 has an infinite volume, it is impossible to solve Eq. (1) numerically. So, we use the following idea: We can consider that the total electric field $\boldsymbol{E}(\boldsymbol{x})$ in the metallic screen will be close to the field inside the metallic (dielectric) screen (slab) without aperture at points far away from the aperture. The field inside the dielectric slab without an aperture can be obtained analytically by solving the well-known problem of reflection and transmission by the two-dimensional dielectric slab. We denote this field by $\boldsymbol{E}^{\mathrm{slab}}(\boldsymbol{x})$ and call slab-field in this paper. Namely, we use the following assumption for the electric field inside the metallic screen as

$$\boldsymbol{E}(\boldsymbol{x}) = \boldsymbol{E}^{\mathrm{C}}(\boldsymbol{x}) + \boldsymbol{E}^{\mathrm{slab}}(\boldsymbol{x}). \quad \boldsymbol{x}\in V_1 \quad \cdots\cdots(3)$$

It is possible to expect that the field denoted by $\boldsymbol{E}^{\mathrm{C}}(\boldsymbol{x})$ in Eq. (3) will be confined in the vicinity of the aperture. We neglect the effects of surface waves that propagate along the screen surface, because the dielectric is dissipative. Substituting Eq. (3) into Eq.(1), we can obtain following equation:

$$\boldsymbol{E}^{\mathrm{C}}(\boldsymbol{x}) + \boldsymbol{E}^{\mathrm{slab}}(\boldsymbol{x}) = k_0^2(n_1^2-1)\iiint_{V_1} \underline{G}_e(\boldsymbol{x}|\boldsymbol{x}')\cdot\boldsymbol{E}^{\mathrm{C}}(\boldsymbol{x}')\mathrm{d}v' + k_0^2(n_1^2-1)\iiint_{V_1} \underline{G}_e(\boldsymbol{x}|\boldsymbol{x}')\cdot\boldsymbol{E}^{\mathrm{slab}}(\boldsymbol{x}')\mathrm{d}v' + \boldsymbol{E}^i(\boldsymbol{x}). \quad \cdots\cdots(4)$$

We notice that slab-field $\boldsymbol{E}^{\mathrm{slab}}(\boldsymbol{x})$ satisfy the volume integral equation as

$$k_0^2(n_1^2-1)\iiint_{V_1+V_a} \underline{G}_e(\boldsymbol{x}|\boldsymbol{x}')\cdot\boldsymbol{E}^{\mathrm{slab}}(\boldsymbol{x}')\mathrm{d}v' + \boldsymbol{E}^i(\boldsymbol{x}) = \boldsymbol{E}^{\mathrm{slab}}(\boldsymbol{x})[\boldsymbol{x}\in V_1] \quad \boldsymbol{E}^t(\boldsymbol{x})[\boldsymbol{x}\in(\mathrm{II})], \quad \cdots\cdots(5)$$

where V_a represents the volume region of the aperture shown in Fig. 1 and $\boldsymbol{E}^t(\boldsymbol{x})$ represents the transmitted plane wave in the upper region (II) above the metallic slab. The fields $\boldsymbol{E}^{\mathrm{slab}}(\boldsymbol{x})$ and transmitted plane wave $\boldsymbol{E}^t(\boldsymbol{x})$ can be expressed analytically. Substituting Eq. (5) into Eq. (4), we can derive the volume integral equation for the field $\boldsymbol{E}^{\mathrm{C}}(\boldsymbol{x})$ only as

$$\boldsymbol{E}^{\mathrm{C}}(\boldsymbol{x}) = k_0^2(n_1^2-1)\iiint_{V_1} \underline{G}_e(\boldsymbol{x}|\boldsymbol{x}')\cdot\boldsymbol{E}^{\mathrm{C}}(\boldsymbol{x}')\mathrm{d}v' - k_0^2(n_1^2-1)\iiint_{V_a} \underline{G}_e(\boldsymbol{x}|\boldsymbol{x}')\cdot\boldsymbol{E}^{\mathrm{slab}}(\boldsymbol{x}')\mathrm{d}v'. \quad \cdots\cdots(6)$$

Comparing Eq. (6) with original volume integral equation (1), we can see that the unknown function i.e., total filed $\boldsymbol{E}(\boldsymbol{x})$, in Eq. (1) is replaced by the field denoted by $\boldsymbol{E}^{\mathrm{C}}(\boldsymbol{x})$ in Eq. (6) and the incident wave $\boldsymbol{E}^i(\boldsymbol{x})$ in Eq. (1) is replaced by the volume integration of slab-filed through the region V_a in Eq. (6). So, the basic structure of Eq. (6) is same as that of Eq. (1). When an aperture in the screen disappears, the last term of right-hand side of Eq. (6) disappears and the solution of Eq. (6) is given by $\boldsymbol{E}^{\mathrm{C}}(\boldsymbol{x})=0$. So, the slab-field $\boldsymbol{E}^{\mathrm{slab}}(\boldsymbol{x})$ becomes the rigorous solution of the problem without an aperture from Eq. (3).

Since we can consider that the field denoted by $\boldsymbol{E}^{\mathrm{C}}(\boldsymbol{x})$ in the screen becomes negligibly small at points far away from the aperture, we can regard the infinite-sized volume integral region V_1as the finite-sized volume region in Eq. (6) and we can solve the integral equation (6) numerically.

Once the electric field denoted by $\boldsymbol{E}^{\mathrm{C}}(\boldsymbol{x})$ in the metallic screen have been obtained numerically, the total electric field in the upper region (II) above the metallic screen can be obtained as

$$\begin{aligned}\boldsymbol{E}(\boldsymbol{x}) &= k_0^2(n_1^2-1)\iiint_{V_1} \underline{G}_e(\boldsymbol{x}|\boldsymbol{x}')\cdot[\boldsymbol{E}^{\mathrm{C}}(\boldsymbol{x}')+\boldsymbol{E}^{\mathrm{slab}}(\boldsymbol{x})]\mathrm{d}v'+\boldsymbol{E}^i(\boldsymbol{x}),\\ &= k_0^2(n_1^2-1)\iiint_{V_1} \underline{G}_e(\boldsymbol{x}|\boldsymbol{x}')\cdot\boldsymbol{E}^{\mathrm{C}}(\boldsymbol{x}')\mathrm{d}v'\\ &\quad - k_0^2(n_1^2-1)\iiint_{V_a} \underline{G}_e(\boldsymbol{x}|\boldsymbol{x}')\cdot\boldsymbol{E}^{\mathrm{slab}}(\boldsymbol{x}')\mathrm{d}v'+\boldsymbol{E}^t(\boldsymbol{x}). \quad \cdots\cdots(7)\end{aligned}$$

In the derivation of Eq. (7), we used the relation Eq. (4) for the slab-field.

The scattered far-field by the aperture in the screen without transmitted plane wave can be expressed as

$$\boldsymbol{E}^s(\mathrm{r},\theta,\phi) \simeq \exp(-jk_0 r)/(k_0 r)\boldsymbol{F}(\theta,\phi), k_0 r \gg 1 \quad \cdots\cdots(8)$$

where $\boldsymbol{F}(\theta,\phi)$ is the scattering coefficient and can be written as

$$\boldsymbol{F}(\theta,\phi) = jk_0^2\zeta/(4\pi)\boldsymbol{i}_r\times\boldsymbol{i}_r\times[k_0^2(n_1^2-1)\iiint_{V_1}\boldsymbol{E}^{\mathrm{C}}(\boldsymbol{x}')\exp(jk_0\boldsymbol{x}'\cdot\boldsymbol{i}_r)dv' - k_0^2(n_1^2-1)\iiint_{V_a}\boldsymbol{E}^{\mathrm{slab}}(\boldsymbol{x}')\exp(jk_0\boldsymbol{x}'\cdot\boldsymbol{i}_r)dv'] \quad \cdots\cdots(9)$$

where polar coordinates (r, θ, ϕ) is shown in Fig. 1 and $\boldsymbol{i}_r$ is a unit vector in the radial direction in the polar coordinates and $\zeta=(\mu_0/\varepsilon_0)^{1/2}$. The total scattering cross section of the aperture can be calculated as

$$W=\int_0^{\pi/2}\int_0^{2\pi}|\boldsymbol{F}(\theta,\phi)|^2\sin\theta d\theta d\phi. \quad \cdots\cdots(10)$$

We can regard W as the scattering power by the aperture in the metallic screen into the region (II) for the case of incident plane wave of unit amplitude.

3. Numerical Calculation

In this paper, we first fix the parameters as follows: The wavelength is λ=488nm, incident angle is $\theta_i=\phi_i=0.0$ (vertical incidence), the incident electric vector $\boldsymbol{E}^i(x)$ is parallel to the x-axis with unit amplitude ($|\boldsymbol{E}_0|=1$), aperture size is $k_0a_x=k_0a_y=1.2$ (about 0.19×0.19 wavelength), complex permittivity of the metal slab is given by $\varepsilon_1=n_1^2 = -1.68 - j4.46$ (Gold) [18]. We discritized the volume integral equation (5) by the pulse function plus point matching (collocation) method and solve the resultant system of linear equations by the iteration method called Generalized Minimum Residual Method (GMRES) [17]. Since the maximum number of unknowns of the linear equations can exceed 10^5, the direct solver such as LU decomposition cannot be used. The finite-sized volume integral region of $V_1=b_x\times b_y\times w$ with the aperture was used in the practical numerical calculation of Eq. (6) shown in Fig.1.

In order to confirm the numerical values obtained, we derived the reciprocity relation for the problem shown in Fig. 1. We first define vectors $\boldsymbol{R}_1$, $\boldsymbol{T}_1$, $\boldsymbol{R}_2$, and $\boldsymbol{T}_2$ by the relation as

$$\boldsymbol{E}^t_j(x)=\boldsymbol{T}_j \exp[-jk_0(x\sin\theta_j\cos\phi_j+y\sin\theta_j\cos\phi_j+z\cos\theta_j)] \quad \cdots\cdots (11)$$

$$\boldsymbol{E}^r_j(x)=\boldsymbol{R}_j \exp[-jk_0(x\sin\theta_j\cos\phi_j+y\sin\theta_j\cos\phi_j-z\cos\theta_j)], \quad (j=1,2)\cdots\cdots(12)$$

where $\boldsymbol{E}^t_j(x)$, and $\boldsymbol{E}^r_j(x)$ denote the transmitted and reflected plane waves by the dielectric slab without an aperture with incident angles of (θ_j, ϕ_j)(j=1,2). Using Maxwell's equations, Eqs. (5), (8) and (12), we can derive the following reciprocity relation as

$$\boldsymbol{R}_1\cdot\boldsymbol{F}_2(\pi-\theta_1,\phi_1)+\boldsymbol{T}_1\cdot\boldsymbol{F}_2(\theta_1,\phi_1)$$
$$=\boldsymbol{R}_2\cdot\boldsymbol{F}_1(\pi-\theta_2,\phi_2)+\boldsymbol{T}_2\cdot\boldsymbol{F}_1(\theta_2,\phi_2) \quad \cdots\cdots (13)$$

In Eq.(13), $\boldsymbol{F}_1(\theta,\phi)$ and $\boldsymbol{F}_2(\theta,\phi)$ represent the scattering coefficients given by Eq. (8) for the case of incident angle of (θ_1, ϕ_1) and (θ_2, ϕ_2), respectively. Since the derivation of Eq. (13) is not difficult and is straightforward, it is omitted in this paper. The results of Eq. (13) are shown in Table 1 for the case of $\phi_1=0$, $\phi_2=0$.

From Table 1, we can confirm that numerical values obtained satisfy the reciprocity relation Eq. (13) within the accuracy of 2-3 effective digits. This result shows that the computer-code does not contradict to Maxwell's equations.

We have confirmed the numerical results by observing the invariance of the results on the volume integral region V_1 used in the numerical calculation. Since the solution of Eq. (6) must be that of the infinitely large metallic screen, the numerical results must be independent of the volume integral region V_1 used in the numerical calculation. In Fig. 2 and 3, near-field distributions $|E_x|^2$ and $|E_z|^2$ obtained on the line parallel to the x-axis ($k_0y=0$, $k_0z=0.1$) are shown with the size of volume integration size $b_x=b_y$ as a parameter. In these results, the thickness of the slab is given by $k_0w=0.3$ and $|E_y|^2$ was omitted because it was small compared with $|E_x|^2$ and $|E_z|^2$. From these figures, when the size of the volume integral region V_1 is greater than that given by about $k_0b_x=k_0b_y=11.2$, we can see that near-field distribution become be independent of the size of the volume integration region V_1. This result also shows the validity of the mathematical formulation in this paper and of our code.

Table 1. Verification of numerical results by reciprocity

θ_1= 0.0 θ_2= 10.0	
LHS of Eq. (13) =	−0.028228+j0.045532
RHS of Eq. (13) =	−0.030675+j0.046152
θ_1= 0.0 θ_2= 20.0	
LHS of Eq. (13) =	−0.022155+j0.040944
RHS of Eq. (13) =	−0.029433+j0.044629

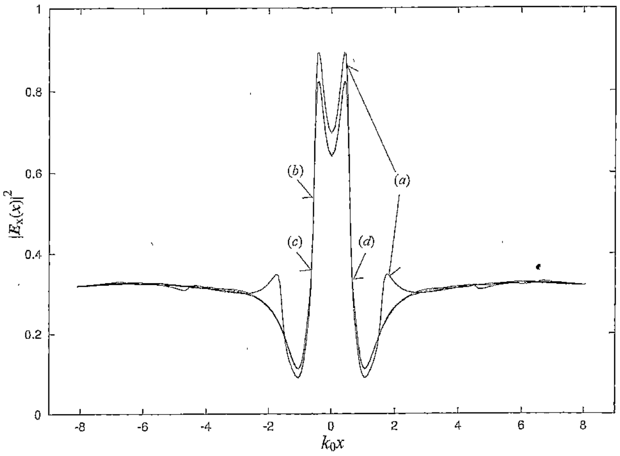

Fig. 2. Dependence of near-field distribution $|E_x(k_0x, 0, 0.1)|^2$ on the size of the region V_1 used in the numerical calculation [(a) $k_0b_x=k_0b_y=3.2$, (b) $k_0b_x=k_0b_y=9.2$, (c) $k_0b_x=k_0b_y=11.2$, (d) $k_0b_x=k_0b_y=13.2$]

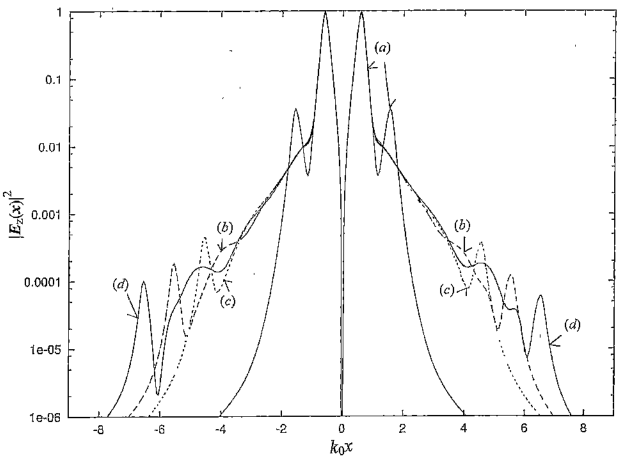

Fig. 3. Dependence of near-field distribution $|E_z(k_0x, 0, 0.1)|^2$ on the size of the region V_1 used in the numerical calculation [(a) $k_0b_x=k_0b_y=3.2$, (b) $k_0b_x=k_0b_y=9.2$, (c) $k_0b_x=k_0b_y=11.2$, (d) $k_0b_x=k_0b_y=13.2$]

4. Throughput

The dependence of scattered power (throughput) of the aperture on the thickness of the metallic screen (slab) is the most interesting information in the NFO technology. The dependence of total scattering cross section W can be regarded as the throughput of far-fields and its dependence on the screen thickness k_0w is shown in Fig. 4. In Fig. 4, the power transmission coefficient of the screen without aperture for incident wave of unit amplitude, i.e., $|T|^2$ and Bethe's results of total scattering cross section are shown. We can find that there is a thickness that gives maximum throughput of the far-fields i.e., $k_0w \approx 0.9$ in Fig. 4 and it will be related to the skin-depth of the material of the metallic screen. The maximum value of W is close to Bethe's result. When the thickness of the screen becomes much larger than the skin depth of the screen, the throughput W becomes smaller than Bethe's result. Bethe's results treated the case of infinitly thin screen of perfect conductor. Since the aperture in this paper is a cutoff waveguide and optical field must decay inside the aperture for the case where the screen is sufficiently thick, this result is physically reasonable. So, the thickness of the screen must be carefully designed in the practical application

5. Field Distributions Above Aperture

Total field distributions in Fig. 5 represents that on the line parallel to the incident electric vector i.e., parallel to the x-axis and $k_0y=0$, $k_0z=0.1$, with thickness as a parameter and those in Fig. 6 represents that on the line perpendicular to the incident electric vector i.e., parallel to the y-axis and $k_0x=0.0$, $k_0z=0.1$, with thickness as a parameter. The near-field intensity of the aperture decreases according to the increase of the thickness of the screen. When the thickness of the screen is rather large, the distribution of the total electrical near-field can be approximated by the two-peaks distribution along x-axis and by the single-peak distribution along the y-axis as shown in Figs. 5 and 6. It is also found that the size of the near-field distribution, that determine the resolution of the NSOM images, cannot be reduced by the increase of the thickness of the screen in the range of practical thickness of the metallic screen.

Distributions of total electric near-field $|\boldsymbol{E}(k_0x, k_0y, 0.1)|^2$ of thin metallic screen of $k_0w=0.3$ (about 0.02 wavelength) and that of thick metallic screen of $k_0w=1.7$ (about 0.27 wavelength) are shown in Figs. 7and 8, respectively. They are distributions of the plane that is parallel to the x-y plane of $k_0z=0.1$ (about 0.02 wavelength) above the screen. We found that basic characteristics of the results of thin screen are rather similar to those of Bethe's result that are results of infinitely thin perfect conductor. However, results of thick metallic screen are slightly different from those of Bethe's results.

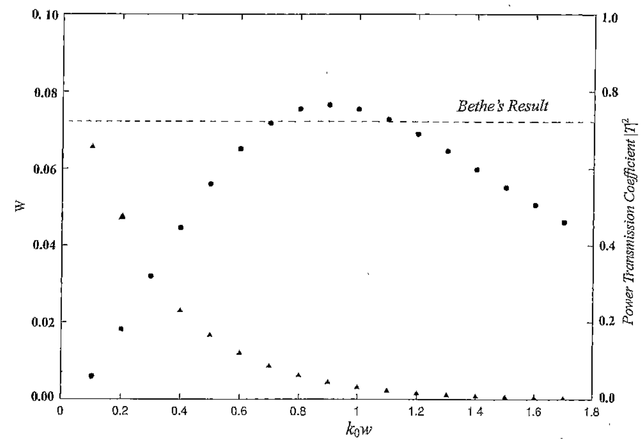

Fig. 4. Dependence of the total cross section W of the aperture on the thickness of the metallic screen k_0w (solid circle). The power transmission coefficient of plane wave of the metallic slab without aperture $|T|^2$ and is also shown by solid triangular

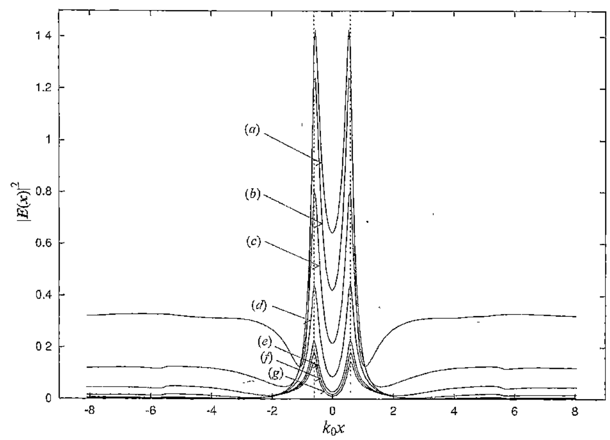

Fig. 5. Near-field distribution of total field $|\boldsymbol{E}(k_0x, 0.0, 0.1)|^2$ along the line parallel to the x-axis [(a) $k_0w=0.3$, (b) $k_0w=0.6$, (c) $k_0w=0.9$, (d) $k_0w=1.2$, (e) $k_0w=1.5$, (f) $k_0w=1.6$, (g) $k_0w=1.7$]

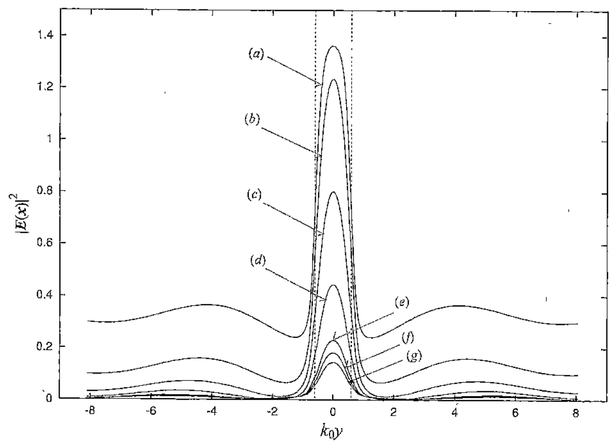

Fig. 6. Near-field distribution of total field $|\boldsymbol{E}(0.0, k_0y, 0.1)|^2$ along the line parallel to the y-axis [(a) $k_0w=0.3$, (b) $k_0w=0.6$, (c) $k_0w=0.9$, (d) $k_0w=1.2$, (e) $k_0w=1.5$, (f) $k_0w=1.6$, (g) $k_0w=1.7$]

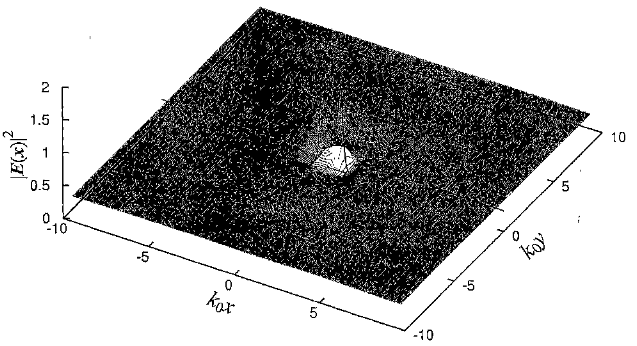

Fig. 7. Near-field distribution of total field $|E(k_0x, k_0y, 0.1)|^2$ on the plane placed parallel to the x-y plane above the screen of the thin screen of k_0w=0.3. Small square indicates the shape of the aperture and large square indicates the volume size of V_1 used in the numerical calculation.

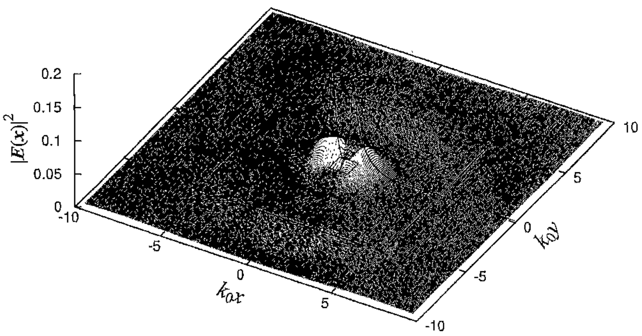

Fig. 8. Near-field distribution of total field $|E(k_0x, k_0y, 0.1)|^2$ on the plane placed parallel to the x-y plane above the screen of the thick screen of k_0w=1.7. Small square indicates the shape of the aperture and large square indicates the volume size of V_1 used in the numerical calculation.

6. Conclutions

The scattering of optical wave by a small aperture in the thick metallic screen has been analyzed by the volume integral equation with effective iteration technique. The near-field distribution in the aperture of the thick metallic screen is slightly different from that of Bethe's result. These results will give very important information in the technology of near-field optics.

When the small object is placed in the vicinity of the aperture and move the object along the metallic screen, we can simulate the NFO microscope. This problem is under consideration.

(Manuscript received Feb.7, 2002, revised Aug.5, 2002)

References

(1) E. Betzig and R. J. Chichester : "Single molecules observed by near-field scanning optical microscopy", *SCIENCE*, **262** pp.1422-1425 (1993-11)

(2) E.H. Synge : "A suggested method for extending microscopic resolution into the ultra-microscopic region", *Phil. Mag*, **6**, pp.356-362 (1928)

(3) H. A Bethe : "Theory of diffraction by small holes", *Phys. Rev.*, **66**, No.7 (1944)

(4) D.W.Pohl and D.Courjon, ed. : Near Field Optic, Kluwer Academic (1993)

(5) M.Ohtsu and H. Hori : Near-Field Nano-Optics, Kluwer Academic/Plenum Publishers, New York (1999)

(6) H. Levine and J. Schwinger : "On the theory of diffraction by an aperture in an infinite plane screen. I", *Phys. Rev.*, **74**, No.8, pp 958-974 (1948)

(7) C. J. Bouwkamp : "On the diffraction of electromagnetic waves by small circular disks and holes", *Philips Res. Rep.*, **5**, pp.401-422 (1950)

(8) Y. Leviatan, R. F. Harrington, and J. R. Mautz : "Electromagnetic transmission through apertures in a cavity in a thick conductor", *IEEE Trans. Antennas Propagat.*, **AP-30**, No.6, pp.1153-1165 (1982)

(9) Y. Leviatan : "Study of near-zone fields of a small aperture", *J. Appl. Phys* **60**, No.5, pp.1577-1583 (1986)

(10) C. M. Butler, Y. Rahma-Samii, and R. Mittra : "Electromagnetic penetration through apertures in conducting surface", *IEEE Trans. Antennas Propagat.*, **AP-26**, No.1, pp 82-93 (1978)

(11) A. Roberts : "Nera-zone fields behind circular apertures in thick, perfectly conducting screens", *J. Appl. Phys.* **65**, No.8, pp 2896-2899 (1989)

(12) A. Roberts : "Small-hole coupling of radiation into a near-field probe", *J. Appl. Phys.*, **70**, No.8, pp.405-4049 (1991)

(13) H. Furukawa and S. Kawata : "Analysis of image formation in a near-field scanning opticalmicroscope· effects of multiple scattering", *Opt. Commun*, **132**, pp 170-178 (1996)

(14) R. Chang, P-K. Wei, W. S. Fann, M. Hayashi, and S. H Lin : "Theoretical investigation of near-field optical propertied of tapered fiber tips and single molecule fluorescence", *J. Appl. Phys.*, **81**, No.8, pp.3369-3376 (1997)

(15) A Chavez-Pison and S. K. Chu : "Afull vector analysis of near-field luminescence probing of singlr quantum dot", *Appl. Phys. Lett.*, **74**, No 11, No.1507-1509 (1999)

(16) O. J F. Martin : "3D simulations of the experimental signal measured in near-field optical microscopy", *J. Microsc*, **194**, pp.235-239 (1999-5/6)

(17) K. Tanaka, M. Yan, and M. Tanaka : "A simulation of near-field optics by three dimensional volume integral equation of classical electromagnetic theory", *Opt. Rev.*, **8**, No.1, pp.43-53 (2001)

(18) E. D Plik : Handbook of Optical Constants of Solid, p 294, Academic Press Handbook Series (1985)

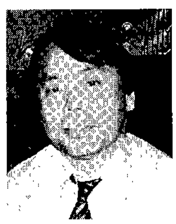

Kazuo Tanaka (Member) received the B.E, M.S., and Ph.D., degrees from the Department of Communications Engineering, Osaka University, Osaka, JAPAN in 1970, 1972 and 1975, respectively. In 1975, he became a Research Associate in the Department of Electrical Engineering at Gifu University. He was an associate Professor in the Department of Electronics and Computer Engineering there in 1985 and in 1990 he was named Professor. His research since 1970 has been a general-relativistic electromagnetic theory and application, radiographic image processing and computational electromagnetics and he is currently interested in the CAD of integral optical circuits, near-field optical circuits and simulation of Anderson localization hypothesis of ball-lightning. He was a visiting Professor of University of Toronto, Canada in 1994. In 1987, he was awarded the Uchida Paper Award by the Japan Society of Medical Imaging and Information Science. He is now a chair of Technical Group of Electromagnetic Theory of IEICE in Japan.

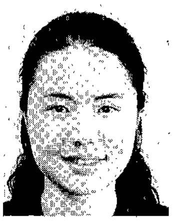

Mengyun Yan (Non-member) received the B.S. degree from the Department of Computer Science, Fudan University, P.R.China in 1990. She worked in Fujian Electrical Computer Corporation as a software engineer from 1990 to 1998. In 1994, she received the Master's degree from Department of Economic, Kagawa University, Japan. She received M.S. degree from the Department of Electrical and Computer Engineering, Gifu University, Japan in 2001, and is currently working towards the Ph.D. degree. Her research interest is the CAD of near-field optical circuits.

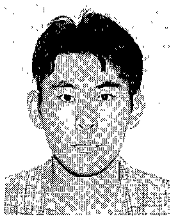

Masahiro Tanaka (Non-member) received the B.E. and M.S. degrees from the Department of Electrical and Computer Engineering, Gifu University, Gifu, JAPAN in 1992 and 1994, respectively. He was a Research Associate at Tokoha-Gakuen Hamamatsu University from 1994 to 1996. He joined Gifu University as a research assistant in 1996. He was a visiting researcher at the Department of Electrical and Computer Engineering, The University of Arizona, USA from 1997 to 1998. His research interests are the CAD of optical waveguide circuits and near-field optical circuits.